

# Comparative Analysis of Linear and Nonlinear Control Strategies for Grid-tie Inverter in PV based Distributed Generation System

Rizwan Nadeem Shah<sup>1\*</sup>, Muhammad Jamil<sup>2</sup>, Khuram Shahzad<sup>3</sup>, Abdul Basit<sup>4</sup>

<sup>1234</sup>US Pakistan Center for Advance Studies in Energy, University of Engineering and Technology Peshawar  
rshah27@asu.edu<sup>1\*</sup>, engrjamil.iub@gmail.com<sup>2</sup>, kshahza1@asu.edu<sup>3</sup>, abdul.basit@uetpeshawar.edu.pk<sup>4</sup>

Received: 14 August, Revised: 20 August, Accepted: 22 August

**Abstract**—In this paper five different control strategies for grid-tie inverter in PV based DG systems have been implemented in MATLAB/Simulink for comparative analysis purpose to evaluate the performance. The control strategies are “Inner loop PI controller with outer loop PI controller in NRF”, “Inner loop PI controller with outer loop PI controller in SRF”, “Inner loop PR controller with outer loop PI controller”, “Inner loop Hysteresis controller with outer loop PI controller”, “Inner loop Repetitive controller with outer loop PI controller”. The performance has been evaluated in both static and dynamic conditions and from the results it is evident that PI controller in SRF, PR controller and Repetitive controller perform best in both static conditions as well as in case of disturbances coming in either from PV side or grid side.

**Keywords**—Proportional Integral Controller, Proportional Resonant Controller, Hysteresis Controller, Repetitive Controller, Single Stage PV System.

## I. INTRODUCTION

As PV based DG system are becoming important part of today's electrical power system. The penetration of PV based DG system has increased tremendously. The total installed capacity of PV system has increased to 138GW globally [1]. To make the efficient use of this energy they must be brought on grid. Thus, PV based distributed generation system uses inverter interface extensively for grid integration. Power injection from PV systems into the main grid must be carried out in a controlled manner. But the penetration of PV system at high level has created grid instability issues. The main cause of these issues is the lack of proper control system for inverter. In literature many strategies have been presented for grid-tie inverter to control the output voltage, output current, output power (both active and reactive) and harmonics [2]. According to IEC 61727 2% change in frequency is allowed in 50 Hz system, while according to IEEE Std. 519-1990 total harmonic distortion should be less than 5%. Moreover, individual current harmonics are listed in table 1. IEC 61727 has also given voltage range for the operation of PV system connected to low voltage distribution network as given in table 2. The important parameters that need to be controlled

are DC-link Voltage, otherwise will cause harmonic distortion and output current to inject the required amount of power into the grid.

TABLE 1: IEEE STD. 929-1992 INDIVIDUAL CURRENT HARMONICS

Odd Harmonics	Distortion limit
3 <sup>rd</sup> - 9 <sup>th</sup>	< 4%
11 <sup>th</sup> - 15 <sup>th</sup>	< 2%
17 <sup>th</sup> - 20 <sup>th</sup>	< 1.5%
23 <sup>rd</sup> - 33 <sup>rd</sup>	< 0.6%
Above the 33 <sup>rd</sup>	< 0.3%

TABLE 2: IEC 61627

Voltage Range	Disconnection time (cycles)
V < 50%	5
50% < V < 85%	100
85% < V < 110%	Normal Operation
110% < V < 135%	100
V > 135%	2.5

In [3][5] the control strategies presented in the literature have been reviewed based on design, implementation and performance. Depending upon the system types different types of control schemes have been implemented so far. the classical controllers like Proportional, Proportional-Integral, Proportional-Derivative, and Proportional-Integral-Derivative are the basic controller used in linear systems [3]. In [4] proportional resonant controller has been implemented; proportional resonant controller is the same as the proportional integral controller, but the only difference is the way through which integration takes place in both controllers. In Proportional Resonant controller the integrator integrates the frequencies closest the resonant frequency which exclude the steady state error or phase shift. Nonlinear controllers have shown remarkable operation as compare to conventional controllers, but they have complexity in implementation and design. In [6] slide mode controller has been used for grid tie inverter. It has been used to adjust the output voltage and to control the output current of the inverter. The good thing

about this technique is the ruthless behavior to load disturbances and parameter variation [3]. Therefore, ideal case zero steady state error is achievable. But microprocessors used in the digital system have limited sampling rate which leads to other phenomena called chattering affect which degrades the performance and reduces the efficiency in power electronics interfaced system. In [7-11] current hysteresis control has been presented, this controller because of its accessibility and ease of implementation was popular for integrated DG systems. In this method the error signal is being kept within a band called “Hysteresis band”. Hysteresis controller causes greater harmonic distortion when the bandwidth of the hysteresis band is kept large, however switching losses gets reduced so trade off should be made while designing hysteresis band. Robust control technique is useful to be implemented when there is error in the system modelling. Controller is designed considering the system uncertainties to achieve vigorous and stable performance in the presence of limited errors in the system model. While designing robust controller, excellent benchmark, neat elucidation and limitations need to be defined clearly. Even if the number of variables needs to be controlled are more than one, guaranteed robust performance and stability in the close loop system can be achieved [12]. In [13,14] H infinity controller has been used as a current controller but it requires accurate system model and involve high level of computational complexity and unable to manage non-linear constraints. PC (Predictive controller) can be implemented when accurate model of the system is known for future prediction. It can handle nonlinearities but requires high level of computations to be done with fast digital system. In [15,16] deadbeat control theory has been presented, in this control scheme the differential equations that control the dynamics of the controlled system need to be derived first and discretized. Based on these dynamic equations, the sampling period of the control signal is first calculated in such a way that the state variables got matched with the reference value at the end of the sampling period. In [17,18,19] repetitive controller is used. The principle behind RC comes from the internal model principle. Which states that by entering the cause of a disturbance/reference in closed loop path, it is possible to obtain a good rejection / location. To deduce whether the error has been reduced or eliminated requires the storage of error signal for one period. Therefore, the RC has remained in for nonlinear periodic loads. By nature, RC lacks dynamic response in spite of showing excellent performance against non-linear periodic loads. However, this problem can be eliminated by combining conventional controller with desired transient response in parallel or cascading. Fuzzy control is a method has made it possible to put in use human knowledge and intelligence in an artificial way to control a system. In [20] Fuzzy controller works based on set of predefined rules but inherently lacks performance parameters. In [21] Autonomous controller has been presented; Autonomous systems are capable of performing complex tasks autonomously. The process of autonomy can be improved by applying human intelligence. This system needs further

improvement as engineers are trying to apply human intelligence and knowledge directly with the aim of achieving high level of automation. In [22,23] Neural Network controller has been presented. Neural Network (NN) contains number of artificial neurons connected together which imitate a biological system of the brain. Neural Network is capable of estimating a map of elective characteristics and can achieve a higher defect endurance. NN can train both online and offline when used in a control system [24]. Adaptive control method has the regulation capability of control actions what so ever the operating conditions of the system are. The precise knowledge of system parameters for high performance of the system. Even though, the computational complexity of this control scheme is high [24,25, 26].

In literature the focus has been designing a controller however performance evaluation must be done against different types of disturbances either coming from grid side or PV side before implementing any control strategy. In this research, combination of different control strategies has been used to evaluate the performance against grid side and PV side disturbance to see which controller performs best in both static and dynamic conditions.

## II. MODEL OF SINGLE STAGE PV SYSTEM

Single stage PV system as presented in figure 1 has been modelled in MATLAB/Simulink to evaluate the performance with different control strategies. It consists of 5kW PV array connected to a capacitor at the output which regulates the output voltage of PV array, grid-tie inverter with LCL filter connected to the grid and associated control and pulse generator to drive the switches. To inject high quality of power two parameter must be controlled which are the DC-link capacitor voltage and output current of the inverter. DC-

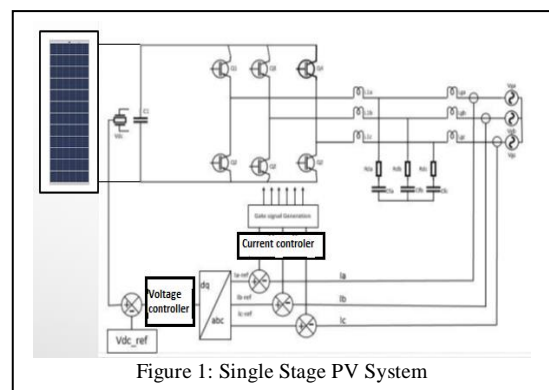


Figure 1: Single Stage PV System

link voltage controller regulates the input voltage by generating reference for the current controller. While current controller regulates the output current of the inverter by following the reference value.

### A. Modelling of PV Array

PV (Photovoltaic) cell has been modelled as a current source in parallel with a resistor as in [33] represented in

Figure 2.  $R_c$  is the shunt resistor while  $R_s$  is the series resistor which represents the resistance of the wire.

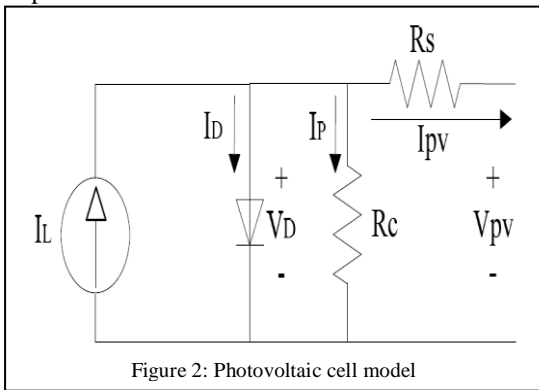


Figure 2: Photovoltaic cell model

5kW PV array has been designed in MATLAB/Simulink using “TRINA SOLAR TSM-250PA05.08” which consists of 60 cells per module. Each Module has 248.86 W at maximum power while there are 22 modules connected in series which generate 700V at the output with 8.06A current. The I-V and P-V curve of 5kW array is shown in Figure 3.

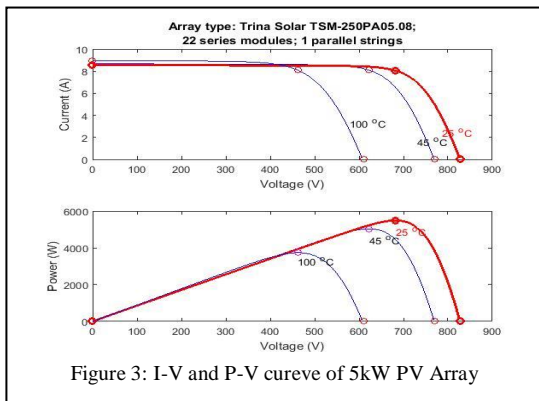


Figure 3: I-V and P-V curve of 5kW PV Array

### B. Modelling of Grid-Tie inverter

Grid tie inverter consist of switching part which is nonlinear and LCL filter which is linear as represented in Figure 4. the dynamic equation of the system can be obtained by applying KCL and KVL to the model. Before that switching function must be defined,

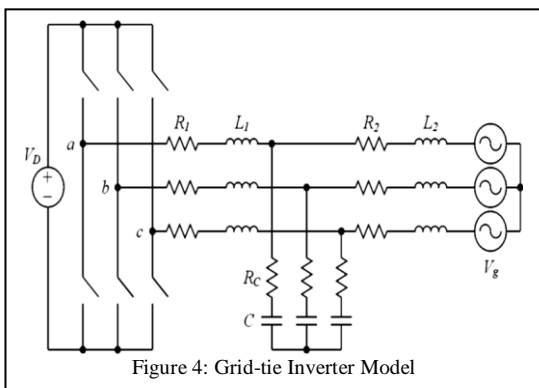


Figure 4: Grid-tie Inverter Model

$$S_i = \begin{cases} 1 & (i_{th} \text{ switch on}) \\ -1 & (i_{th} \text{ switch off}) \end{cases} \quad i = 1, 2 \dots 6 \quad (1.1)$$

$$S_{ak} = \frac{1}{2} + \frac{1}{4}(S_1 - S_2) \quad (1.2)$$

$$S_{bk} = \frac{1}{2} + \frac{1}{4}(S_3 - S_4) \quad (1.3)$$

$$S_{ck} = \frac{1}{2} + \frac{1}{4}(S_5 - S_6) \quad (1.4)$$

Where  $k = 0, 1 \dots 7$ .

The system state model can be obtained by applying KVL and KCL to the per phase model of the LCL filter as represented in Figure 5.

$$\frac{di_1}{dt} = -\left(\frac{R_c + R_1}{L_1}\right)i_1 + \left(\frac{R_c}{L_1}\right)i_2 - \left(\frac{1}{L_1}\right)v_c + \left(\frac{V_D}{2L_1}\right)S \quad (1.6)$$

$$\frac{di_2}{dt} = \left(\frac{R_c}{L_2}\right)i_1 - \left(\frac{R_c + R_2}{L_2}\right)i_2 + \left(\frac{1}{L_2}\right)v_c - \left(\frac{1}{L_2}\right)v_g \quad (1.7)$$

$$\frac{dv_c}{dt} = \left(\frac{1}{C}\right)i_1 - \left(\frac{1}{C}\right)i_2 \quad (1.8)$$

The state vector  $x(t)$  contains inductor current  $i_1(t)$  at the switching side, inductor current  $i_2(t)$  at grid side and the filter capacitor voltage  $v_c(t)$  as state variables in stationary reference frame. For per phase system the state vector  $x(t)$  would become:

$$x(t) = [i_{1a}(t) \ i_{2a}(t) \ v_{ca}(t)]^T \quad (1.9)$$

the continuous time state space model derived from the KVL equations in given below:

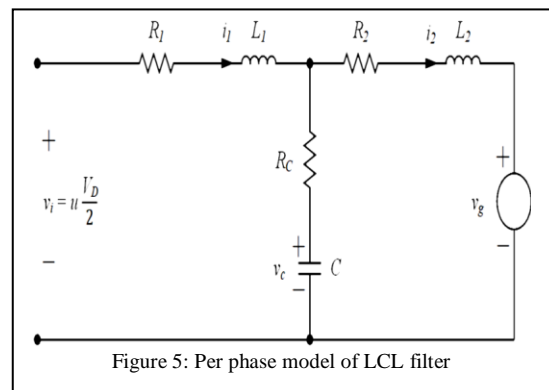


Figure 5: Per phase model of LCL filter

$$\frac{dx(t)}{dt} = Ax(t) + BU(t) + Pg(t) \quad (1.10)$$

$$y(t) = Cx(t) \quad (1.11)$$

Where,

$$A = \begin{bmatrix} \frac{R_c + R_1}{L_1} & \frac{R_c}{L_1} & -\frac{1}{L_1} \\ \frac{R_c}{L_2} & \frac{R_c + R_2}{L_2} & \frac{1}{L_2} \\ \frac{1}{C} & -\frac{1}{C} & 0 \end{bmatrix}, B = \begin{bmatrix} \frac{V_D}{2L_1} \\ 0 \\ 0 \end{bmatrix}, P = \begin{bmatrix} 0 \\ -\frac{1}{L_2} \\ 0 \end{bmatrix},$$

$$C = [0 \ 1 \ 0]$$

### C. Design of LCL filter

LCL filter provides better harmonics attenuation as compared to simple L and LC filter however designing LCL filter is a complex task. The values of L and C must be chosen in such a way that the resonance frequency should be far away from the switching frequency as well as fundamental frequency  $\omega_g \times 10 \leq \omega_{res} \leq 0.5 \times \omega_{sw}$  [27].

$$(\omega_{res})^2 = \frac{L_1 + L_2}{L_1 L_2 C} \quad (1.12)$$

While

$$CL_T = \frac{1}{(\omega_{res})^2 \left( \frac{r_1}{r_1 + 1} \right)^2} \quad (1.13)$$

Where  $L_1 + L_2 = L_T$  and  $r_1 = \frac{L_2}{L_1}$ , thus  $(\omega_{res})^2 = \frac{4}{CL_T}$ . The values of capacitance can't be greater than  $0.05(C_{base})$  By selecting  $\omega_{res} = 2000\pi \text{ rad/sec}$ ,  $r_1 = 1$  and  $C = 5\mu\text{F}$  the value of inductor can be found out  $L_T = 5.1\text{mH}$ . thus  $L_1 = L_2 = 2.55\text{mH}$ . The values of damping resistor can be found out from the following formula.  $R_C = \frac{1}{3\omega_{res}C}$ , Thus  $R_C = 10.6 \Omega$ .

### III. CONTROL STRATEGIES

In order to do performance evaluation five different control strategies have been implemented in MATLAB/Simulink each control strategy contains two controllers, voltage controller that control the voltage across DC-link capacitor and generates reference for current controller, while current controller regulates the grid injected current according the reference value. in each case proportional integral controller has been used as DC-link voltage controller while current controller varies. The implemented control strategies are given below:

#### A. PI DC-link voltage controller with PI current controller in NRF

In this control scheme proportional integral controller regulates the DC-link voltage according the reference value while proportional integral controller in the inner loop regulates the output current. Current controller is implemented in natural reference frame where the current vectors are rotating while reference frame is stationary. While reference current is being generated through Clark's and Park's transformation as given in [28] for current controller. The control block is represented in Figure 6. PI controller is tuned in MATLAB/SISO tool according the required performance parameter such as 20% overshoot, settling time 20ms and zero steady state error.

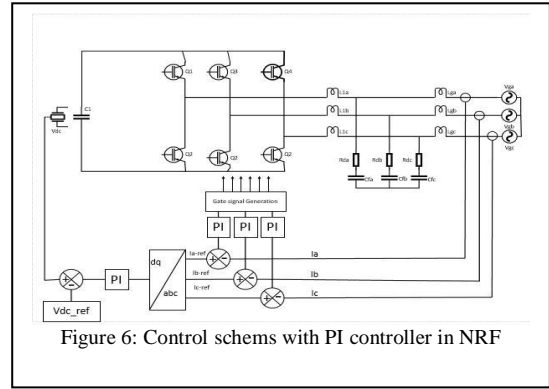


Figure 6: Control schemes with PI controller in NRF

#### B. PI DC-link voltage controller with PI current controller in SRF

In this control strategy DC-link voltage controller is the same PI controller as implemented in A, while PI current controller is implemented in Synchronous reference frame by transforming three phase rotating current vectors into DC form while the reference frame rotates at synchronous speed as in Figure 7. PI controller is tuned by using MATLAB/SISO tool according to the required transient response and steady state error.

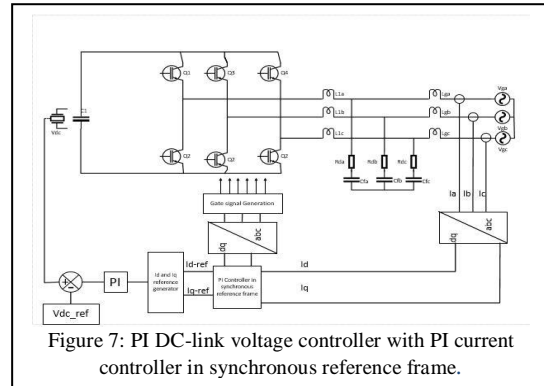


Figure 7: PI DC-link voltage controller with PI current controller in synchronous reference frame.

#### C. PI DC-link voltage controller with PR current controller in NRF

In this control strategy same PI controller has been adopted to control DC-link voltage while Proportional resonant controller controls the output current of the inverter. As the ideal PR controller is difficult to realize that's why improved version as mentioned in [29] has been used. In PR controller the proportional gain remains the same as in PI controller

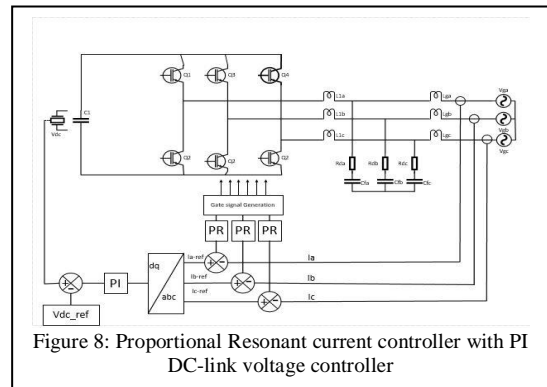


Figure 8: Proportional Resonant current controller with PI DC-link voltage controller

which forms the dynamics of the system according to the bandwidth (gain and phase margin). The values of integral and proportional gains are determined as mentioned in [38]. Figure 8 represents the controller scheme with PR current controller in NRF.

**D. PI DC-link voltage controller with Hysteresis current controller in NRF**

Hysteresis current controller is a non-linear controller and special case of slide mode controller where the error signal is kept within a band called hysteresis band. It inherently lacks transient response parameters. Hysteresis band defines the maximum switching frequency and output error with reference to the reference signal. Hysteresis current controller along with PI controller has been implemented as mentioned in [30] and represented in Figure 9. In this control strategy the transient response parameters are determined solely by PI DC-link voltage controller.

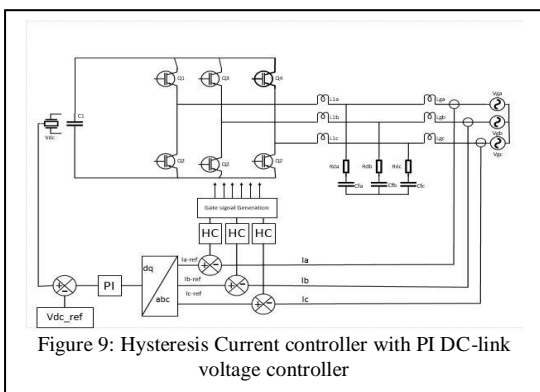


Figure 9: Hysteresis Current controller with PI DC-link voltage controller

**E. PI DC-link voltage controller with Repetitive current controller in NRF**

Repetitive controller has been used for the tracking of periodic signal which mainly works based on internal model principle. RC Controller as mentioned in [31] has been implemented along with Proportional integral DC-link voltage controller as presented in Figure 10. Just like Hysteresis current controller Repetitive current controller also inherently lacks transient response parameters, that's why conventional PI controller is used in cascade to stabilize the plant [32].

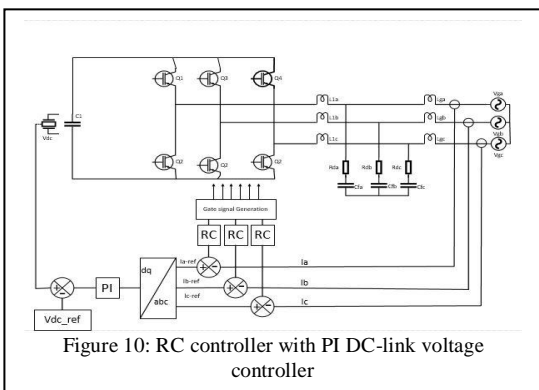


Figure 10: RC controller with PI DC-link voltage controller

**IV. SIMULATION RESULTS**

The Simulation results have been obtained for each control strategy in both static and dynamic conditions to evaluate the performance. In static conditions there is no change in parameters either on the grid side or PV side such that the system operates in ideal conditions. While in dynamic conditions the system performance has been evaluated against different types of disturbances coming either from the PV side or grid side. The possible disturbances on PV side can be the change in irradiance level or temperature which may vary the output power of PV system. While on grid side the disturbance can be in the form of short term voltage dip or voltage swell which can't be detected by the protection system and change in frequency in grid phase angle.

**A. Static conditions**

The response of each control strategy has been shown in this section. In static conditions there is no change of parameter either on grid side or PV side. DC link voltage and reference tracking of current controller in case of each control strategy has been presented in the Figure 11, Figure 12, Figure 13, Figure 14 and Figure 15 below.

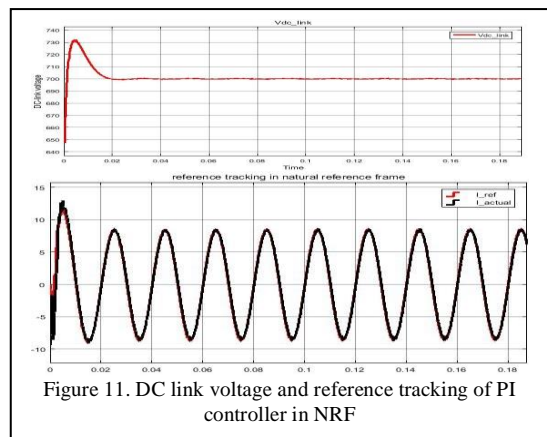


Figure 11: DC link voltage and reference tracking of PI controller in NRF

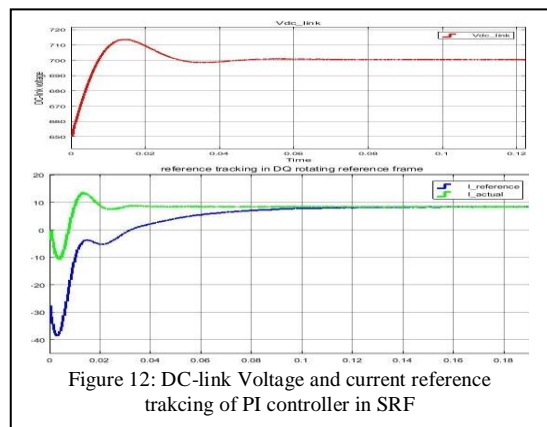
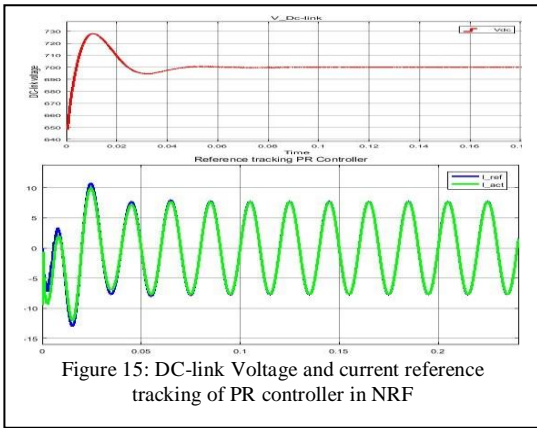
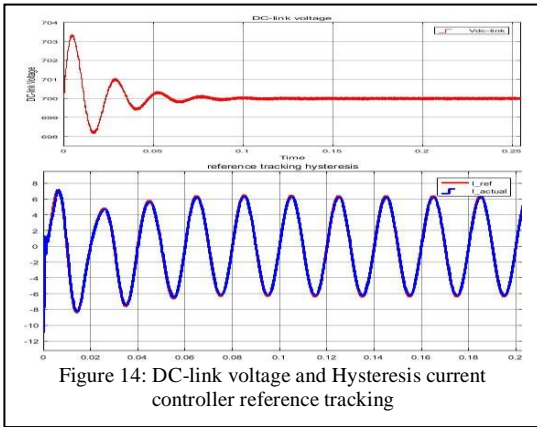
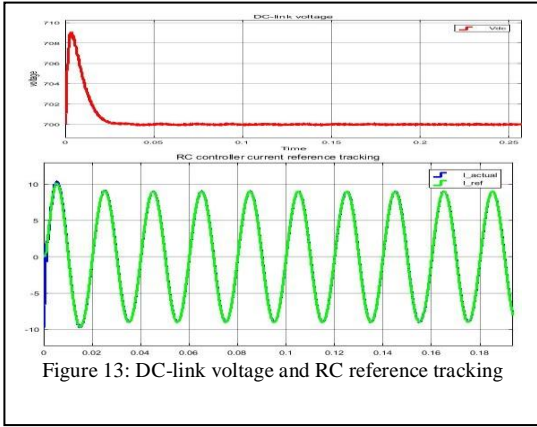
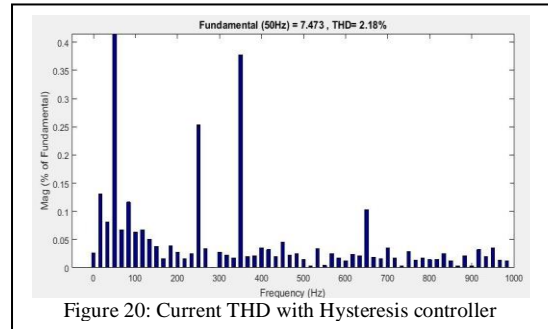
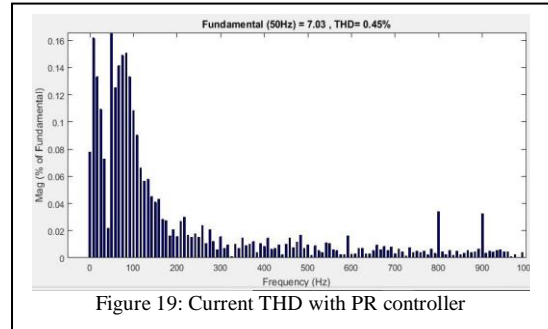
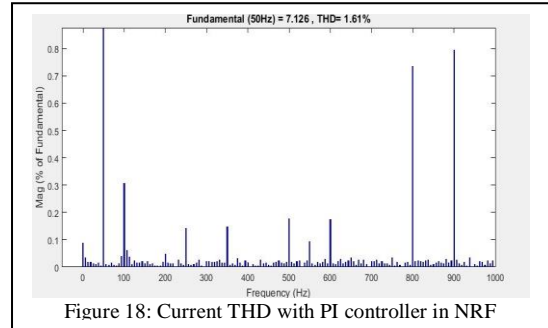
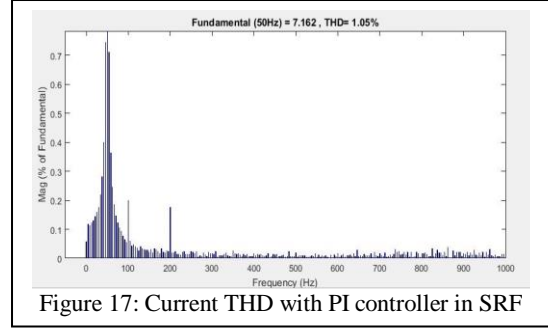
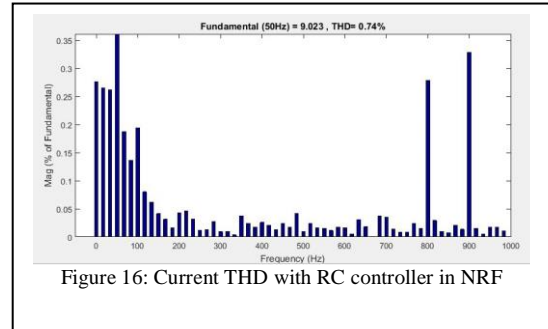


Figure 12: DC-link Voltage and current reference tracking of PI controller in SRF



In static conditions each control strategy perform well as expected. Each controller gets stable according to the preset transient parameters. As it can be seen in Figure 11 the inner loop gets stable first than the outer loop gets stable while the current loop tracks the reference value with zero steady state error. Another important parameter that should be monitored is the total harmonic distortion in the output current that should follow the iee standards. Figure 16 to Figure 20 show the THD in the output current of each control strategy. As it is evident from Figure 20 Hysteresis controller results greater Harmonics as compare to any other control strategy while PR controller results in least Harmonics in the output current as it

is depicting from Figure 19. total harmonic distortion in each case is less than 5%.



### B. Dynamic Conditions

In dynamic conditions the performance has been evaluated against grid side disturbances as well as PV side disturbances. PV side disturbance could be the change in PV output power while on grid side disturbances can be in the form of voltage swell and voltage dip.

#### 1) Reference tracking

To see the reference tracking ability of each control strategy the output power of PV has been changed in different time intervals in dynamic conditions, the results have been shown in Figure 21 to Figure 25.

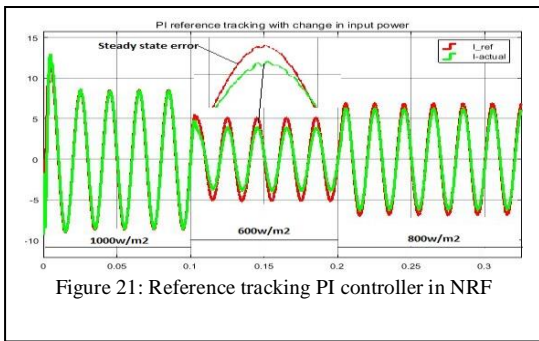


Figure 21: Reference tracking PI controller in NRF

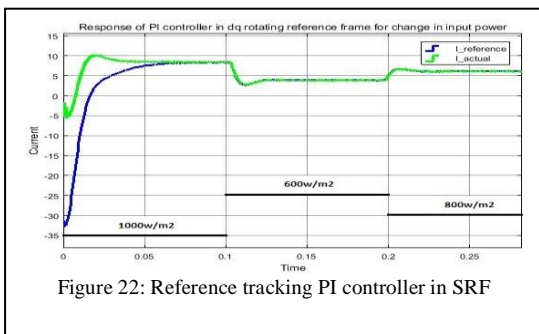


Figure 22: Reference tracking PI controller in SRF

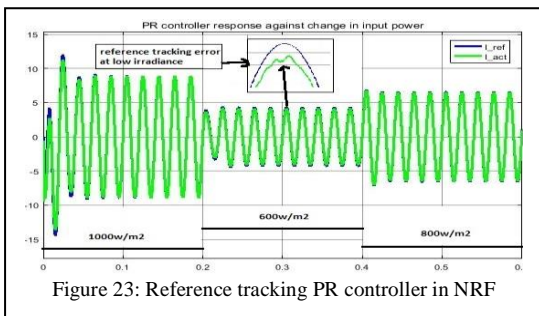


Figure 23: Reference tracking PR controller in NRF

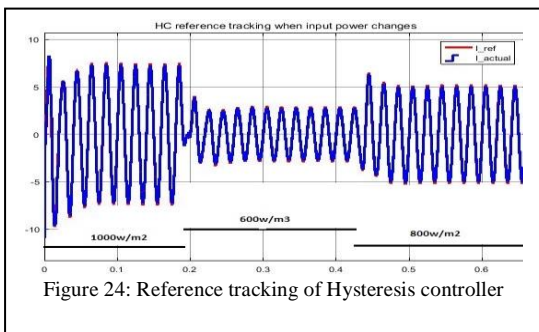


Figure 24: Reference tracking of Hysteresis controller

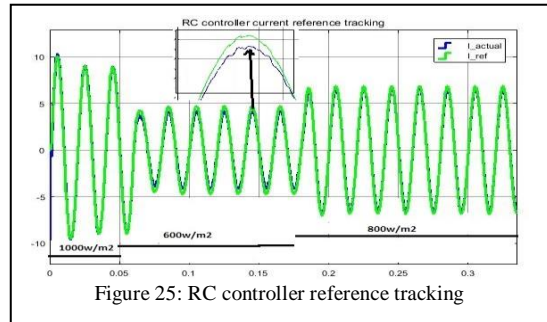


Figure 25: RC controller reference tracking

As it is evident from Figure 21 that PI controller in Natural reference frame is not good reference tracker as it causes steady state error at low irradiance level which is about 25%. So the efficiency of the system will drop at low irradiance level. While PI controller in SRF and Hysteresis controller are good reference trackers with zero steady error as in Figure 22 and 24. While PR controller and RC controller present the same steady state error at low irradiance level as can be seen in Figure 23 and 25.

#### C. Voltage Dip of 0.1pu

Voltage dip is a common phenomenon which can occur because of the connection of a large inductive load and ground faults, so the controller should provide stable operation in case of short-term faults that cannot be sensed by the protection system. Thus, the performance of the implemented control strategies is evaluated for a voltage dip of 5ms. Figure 26 to Figure 30 show the response of each control strategy.

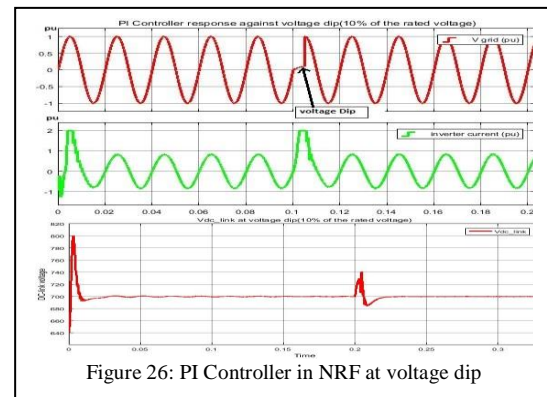


Figure 26: PI Controller in NRF at voltage dip

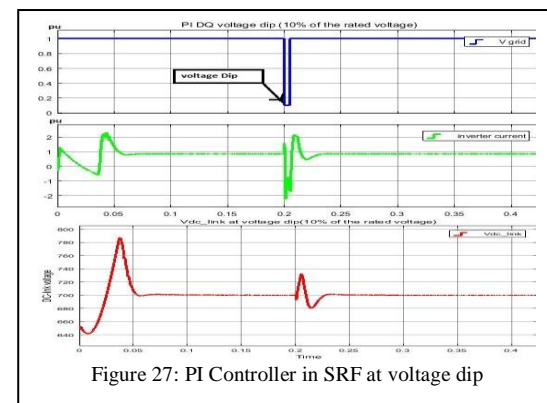


Figure 27: PI Controller in SRF at voltage dip

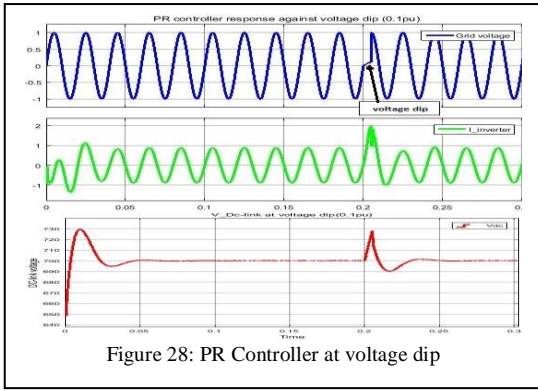


Figure 28: PR Controller at voltage dip

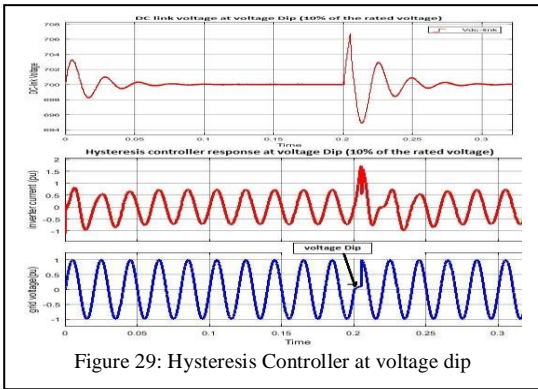


Figure 29: Hysteresis Controller at voltage dip

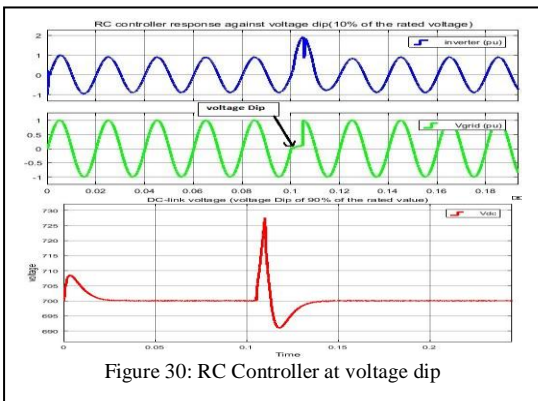


Figure 30: RC Controller at voltage dip

**D. Voltage Swell 1.8 pu**

Voltage swell is common phenomena which can occur as results of disconnection of large inductive load and in resistance grounded system when there is fault in any phase, voltage of the other healthy phases goes high. So controller should provide stable operation in case of short term faults that

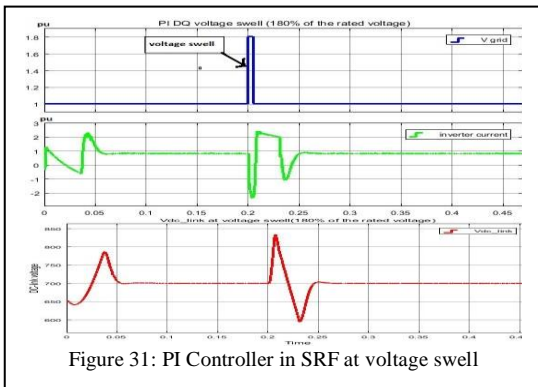


Figure 31: PI Controller in SRF at voltage swell

can't be sensed by the protection system. So, the performance of the implemented control strategies is evaluated for voltage swell of 5ms. Figure 31 to Figure 35 show the response of each control strategy.

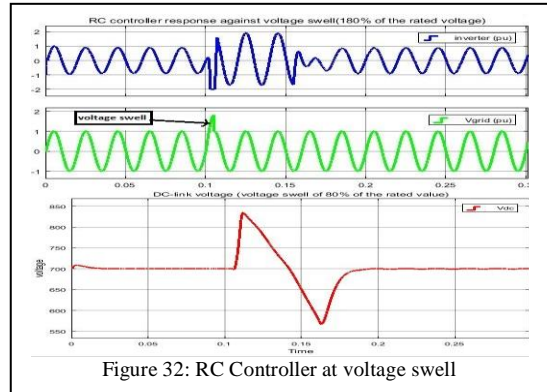


Figure 32: RC Controller at voltage swell

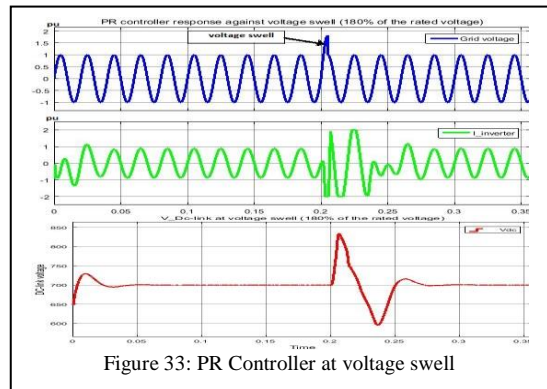


Figure 33: PR Controller at voltage swell

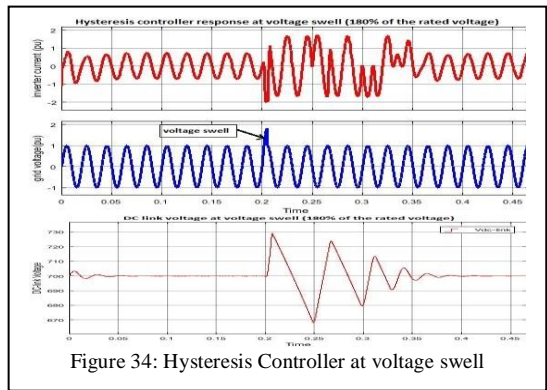


Figure 34: Hysteresis Controller at voltage swell

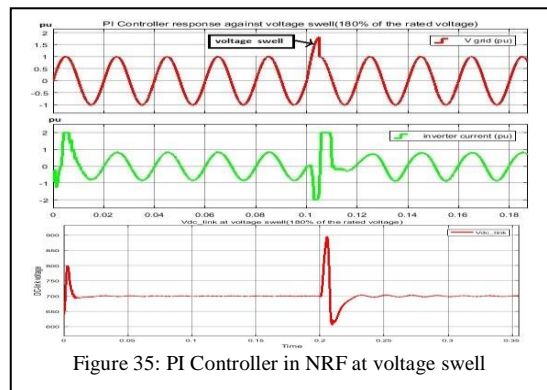


Figure 35: PI Controller in NRF at voltage swell

### E. Power Injection

Single stage PV systems does not have MPPT controller, that's why it is important to evaluate the performance the system efficiency in terms of Power generated by PV system and power injected into the grid. Figure 36 to Figure 40 present the power injection of each control strategy.

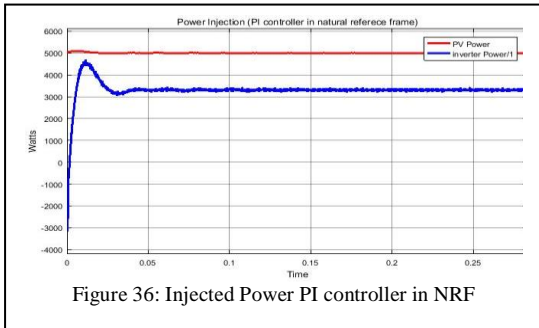


Figure 36: Injected Power PI controller in NRF

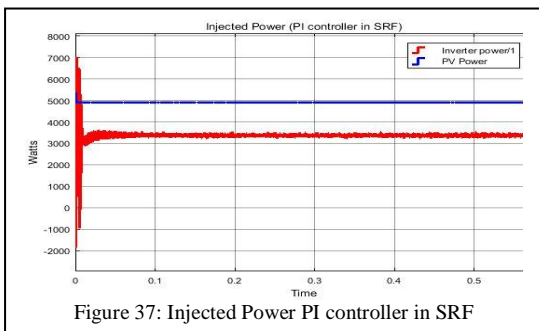


Figure 37: Injected Power PI controller in SRF

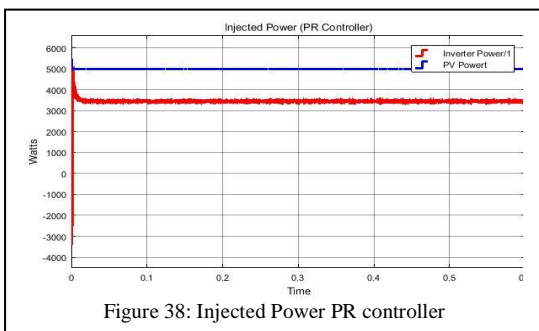


Figure 38: Injected Power PR controller

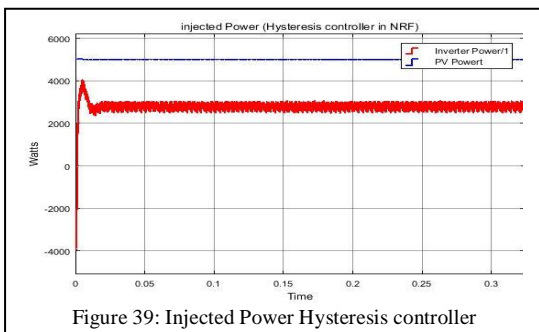


Figure 39: Injected Power Hysteresis controller

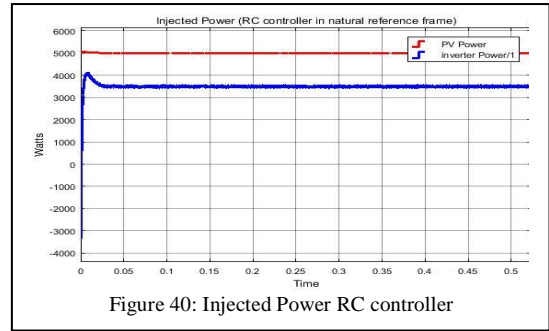


Figure 40: Injected Power RC controller

### V. RESULTS OF THE CASE STUDIES

The results of the case studies run for performance evaluation have been summarized in the below tables to ease the understanding. Table 3 presents the Total Harmonic Distortion in the output current in case of each control strategy. Table 4 presents the time taken by each controller to get stable after the removal voltage dip while table 5 presents the time taken by each controller to get stability after the removal of voltage swell in terms of no of cycles, while table 6 presents the efficiency of the system with different control strategies. As it is evident from table 3 that PI control in natural reference frame offer the least harmonic distortion in the output current while hysteresis controller total harmonic distortion is maximum among all control strategies.

TABLE 3: TOTAL HARMONIC DISTORTION

S.No	Control Strategy	%THD
1	PI DC-link voltage controller, PI current controller in Natural reference frame	1.61
2	PI DC-link voltage controller PI current controller in Synchronous reference frame	1.05
3	PI DC-link voltage controller with Proportional resonant current controller	0.45
4	PI DC-link voltage controller with hysteresis current	2.18
5	PI DC-link voltage controller with repetitive current controller	0.74

TABLE 4: STABILITY TIME AFTER REMOVAL OF FAULT (VOLTAGE DIP)

S.No	Control Strategy	Time (no of cycles)
1	PI DC-link voltage controller, PI current controller in Natural reference frame	1
2	PI DC-link voltage controller with PI current controller in Synchronous reference frame	2
3	PI DC-link voltage controller Proportional resonant current controller	3
4	PI DC-link voltage controller with hysteresis current	5
5	PI DC-link voltage controller with repetitive current controller	1

TABLE 5: STABILITY TIME AFTER REMOVAL OF FAULT (VOLTAGE SWELL)

S.No	Control Strategy	Time (no of cycles)
1	PI DC-link voltage controller with PI current controller in Natural reference frame	1
2	PI DC-link voltage controller with PI current controller in Synchronous reference frame	2
3	PI DC-link voltage controller with proportional resonant current controller	3
4	PI DC-link voltage controller with hysteresis current	10
5	PI DC-link voltage controller with repetitive current controller	3

TABLE 6: EFFICIENCY OF PV SYSTEM WITH DIFFERENT CONTROL STRATEGIES

S.No	Control Strategy	Efficiency
1	PI DC-link voltage controller PI current controller in Natural reference frame	65.8%
2	PI DC-link voltage controller PI current controller in Synchronous reference frame	69.2%
3	PI DC-link voltage controller with proportional resonant current controller	76.8%
4	PI DC-link voltage controller with hysteresis current controller	55.8%
5	PI DC-link voltage controller with repetitive current controller	69.8%

### CONCUSLION

In this paper five different control strategies have been implemented in MATLAB/Simulink for grid-tie inverter in PV based distributed generation system applications. The performance of each control strategy has been evaluated both in static and dynamic conditions to see which controller performs best. As it is evident from the results that PI controller in Synchronous reference frame, PR controller in natural reference frame and RC controller show better performance in terms of reference tracking, stability, THD and efficiency in both static and dynamic conditions, while PI controller natural reference frame causes steady state error at low irradiance level causing efficiency drop. Moreover, hysteresis controller results in high total harmonic distortion in the output current.

### REFERENCES

[1] European Photovoltaic Industry Association, "Global market outlook– for photovoltaics 2014 2018," EPIA, Tech. Rep., Jun. 2014, ISBN 9789082228403.

[2] Ned Mohan, Tore M. Undeland, and William P. Robbins, *Power Electronics*, 2<sup>nd</sup> ed., pp. 23, 241, and 726, John Wiley & Sons, Inc., New York, 1995.

[3] Athari, Hamed, Mehdi Niroomand, and Mohammad Ataei. "Review and classification of control systems in grid-tied inverters." *Renewable and Sustainable Energy Reviews* 72 (2017): 1167-1176

[4] Teodorescu R, Blaabjerg F, Liserre M, Loh PC. Proportional-resonant controllers and filters for grid-connected voltage-source converters. *IEEE Proc Electr Power Appl* 2006;153(5):750–62, [Sept.].

[5] Chatterjee, Aditi, and Kanungo Barada Mohanty. "Current control strategies for single phase grid integrated inverters for photovoltaic applications-a review." *Renewable and Sustainable Energy Reviews* 92 (2018): 554-569.

[6] Komurcugil H. Rotating-sliding-line-based sliding-mode control for single-phase UPS inverters. *IEEE Trans Ind Electron* 2012;59(10):3719–26, [Oct.].

[7] Krismadinata C, Rahim NA, Selvaraj J. Implementation of hysteresis current control for single-phase grid connected inverter. In: *Proceedings 7th International Conference on Power Electronics and Drive Systems, Bangkok*; 2007. p. 1097–1101.

[8] Dahono PA. New hysteresis current controller for single-phase full-bridge inverters. *IET Power Electron* 2009;2(5):585–94.

[9] Yao Z, Xiao L. Control of single-phase grid-connected inverters with nonlinear loads. *IEEE Trans Ind Electron* 2013;60(4):1384–9.

[10] Elsharty MA, Hamad MS, H. A. Ashour HA. Digital hysteresis current control for grid-connected converters with LCL filter. In: - *Proceedings 37th Annual Conference of the IEEE Industrial Electronics Society (IECON), Melbourne, VIZ*; 2011. p. 4685–4690.

[11] Ichikawa R, Funato H, Nemoto K. Experimental verification of single-phase utility interface inverter based on digital hysteresis current controller. In: *Proceedings International Conference on Electrical Machines and Systems*.

[12] Damen A, Weiland S. Robust Control. Measurement and Control Group Department of Electrical Engineering Eindhoven University of Technology P.O. Box 513, Draft version, July 2002.

[13] Zames G. Feedback and optimal sensitivity: model reference transformations, multiplicative seminorms, and approximate inverses. *IEEE Trans Autom Control* 1981:301–20.

[14] Hornik T, Zhong Q Ch. A current-control strategy for voltage-source inverters in microgrids based on  $H_{\infty}$  and repetitive control. *IEEE Trans Power Electron* 2011;26(3), [March].

[15] Abu-Rub H, Guzin'ski J, Krzeminski Z, Toliyat HA. Predictive current control of voltage-source inverters. *IEEE Trans Ind Electron* 2004;51(3), [Jun.].

[16] Moreno JC, Huerta JME, Gil RG, Gonzalez SA. A robust predictive current control for three phase grid-connected inverters. *IEEE Trans Ind Electron* 2009;56(6):1993–2004, [Jun.].

[17] Bojoi R, Limongi LR, Roiu D, Tenconi A. Enhanced power quality control strategy for single-phase inverters in distributed generation systems. *IEEE Trans Power Electron* 2011;26(3):798–806, [March].

[18] de Almeida PM, Duarte JL, Ribeiro PF, Barbosa PG. Repetitive controller for improving grid connected photovoltaic systems. *IET Power Electron* 2014;7(6):1466–74, [June].

[19] Ramos C, Martins A, Carvalho A. Complex state-space current controller for grid connected converters with an LCL filter. In: *35th Annual conference of IEEE industrial electronics, IECON '09*. 2009. pp. 296–301.

[20] Passino KM. Intelligent control: anan overview of techniques. Department of Electrical Engineering, Ohio State University; 2015.

[21] Wang X, Blaabjerg F, Chen Z. Autonomous control of inverter-interfaced distributed generation units for harmonic current filtering and resonance damping in an islanded microgrid. *IEEE Trans Ind Appl* 2014;50(1):452–61, [Jan.- Feb.].

[22] Lin FJ, Ch. Lu K, Ke TH. Probabilistic Wavelet Fuzzy Neural Network based reactive power control for grid-connected three-phase PV system during grid faults. *Renew Energy* 2016;92:437 49, [July].

- [23] Kyoungsoo R, Rahman S. Two-loop controller for maximizing performance of a grid-connected photovoltaic-fuel cell hybrid power plant. *IEEE Trans Energy Convers* 1998;13(3):276–81, [Sep].
- [24] Niroomand M, Karshenas HR. Review and comparison of control methods for uninterruptible power supplies. In: 1st power electronic and drive systems and technologies conference, 2010.
- [25] Eren S, Pahlevani M, Bakhshai A, Jain P. An adaptive droop DC-bus voltage controller for a grid-connected voltage source inverter with LCL filter. *IEEE Trans Power Electron* 2015;30(2):547–60, [Feb.].
- [26] Zhong QC, Hornik T. Control of power inverters in renewable energy and smart grid integration. John Wiley & Sons; 2013.
- [27] M. Liserre, F. Blaabjerg and S. Hansen. "Design and control of an LCL-filter based three-phase active rectifier. Industry Applications, IEEE Transactions vol. 41, no. 5, 1281-1291, 2005.
- [28] Damen A, Weiland S. Robust Control. Measurement and Control Group Department of Electrical Engineering Eindhoven University of Technology P.O. Box 513, Draft version, July 2002.
- [29] Zmood, D.N.; Holmes, D.G. Stationary frame current regulation of PWM inverters with zero steady-state error. *IEEE Trans. Power Electron.* **2003**, *18*, 814–822.
- [30] Wei Gu and Issa Batarseh, "Interleaved synchronous buck regulator with hysteretic voltage control," *2001 IEEE 32 Annual Power Electronics Specialists Conference*, Vol. 3, pp. 1512–1516, 2001.
- [31] Youqing Wang, Furong Gao, and Francis J. Doyle. Survey on iterative learning control, repetitive control, and run-to-run control. *J. Process Control*, 19(10):1589{1600, 2009.
- [32] Yongheng Yang, Keliang Zhou, and Frede Blaabjerg. Harmonics suppression for single phase grid-connected PV systems in different operation modes. 2013 Twenty-Eighth Annu. IEEE Appl. Power Electron. Conf. Expo., pages 889{896, mar 2013.
- [33] Youqing Wang, Furong Gao, and Francis J. Doyle. Survey on iterative learning control, repetitive control, and run-to-run control. *J. Process Control*, 19(10):1589{1600, 2009.
- [34] X. Lu and J. Wang, "A Game Changer: Electrifying Remote Communities by Using Isolated Microgrids," *IEEE Electrif. Mag.*, vol. 5, no. 2, pp. 56–63, 2017.



**Rizwan Nadeem Shah** was born in District Chitral Khyber Pakhtunkwa Pakistan. on 3<sup>rd</sup> April 1990, He has got his bachelor's degree in electrical power engineering from COMSATS Institute of Information Technology Abbottabad Pakistan in 2015, currently he is getting his master's degree in

electrical energy system Engineering from US Pakistan Center for Advanced Studies in Energy, University of Engineering and Technology Peshawar Pakistan. His research interest includes distributed generation, microgrid operation and control.